Equivalence of the analytic mean-field potential approach with free-volume theory and verification of its applicability based on the Vinet equation of state

Sun Jiuxun,[1] Cai Lingcang,[2] Wu Qiang,[2] and Jing Fuqian[2]
[1]*Department of Applied Physics, University of Electronic Science and Technology, Chengdu 610054, China*
[2]*Laboratory for Shock Wave and Detonation Physics Research, Southwest Institute of Fluid Physics, Mianyang 621900, China*
(Received 17 July 2004; revised manuscript received 11 October 2004; published 19 January 2005)

The analytic mean-field potential (AMFP) method proposed by Wang *et al.* (WAMFP) is verified to be equivalent to the free-volume theory. A generalized analytic mean-field potential (GAMFP) is established in terms of the free-volume theory and the nearest-neighbor pairwise interaction assumption. The GAMFP contains an integral. By using numerical integrated formula to approximately evaluate the integral, the GAMFP is transformed to the WAMFP or other forms of the AMFP, and the WAMFP can be seen as an approximate analytic version of the GAMFP. The GAMFP is exact for nearest-neighbor Lennard-Jones (NN-LJ) model solid. The numerical results for thermodynamic quantities of NN-LJ solid from the GAMFP is compared with the WAMFP and other AMFP's with slightly different forms. The comparison shows that the numerical results from the WAMFP are almost completely in agreement with the GAMFP and are better than several other approximate AMFP's. The GAMFP and WAMFP with quantum modification have been applied to Vinet-type solids. The numerical results show that the theoretical values of Grüneisen γ_G and Debye temperature Θ_D for three type solids are qualitatively in agreement with experiments, but the agreement is not satisfactory quantitatively. The predicted values of bulk thermal expansivity are too large for rare-gas solids, too small for alkali halides, and for metallic solids the agreement is slightly better but also is not satisfactory. Especially the predicted variations of bulk thermal expansivity and compressibility versus temperature are fairly bad; except for copper, the prediction is fortunately acceptable. It is shown that the fundamental spirit of the GAMFP and WAMFP to use all cold energy to evaluate thermal properties is in contradiction with embedded-atom model (EAM). It is necessary to improve the GAMFP and WAMFP in terms of the EAM by the replacement of all cold energy with only cold energy from interaction between metallic atoms.

DOI: 10.1103/PhysRevB.71.024107 PACS number(s): 64.10.+h, 05.70.Ce, 65.40.−b

I. INTRODUCTION

Over the past decades, a large amount of progress has been made upon the properties of a material at extreme conditions.[1] In the experimental direction, the most important sources of experimental information on the thermal properties of a material at high pressures and temperatures are dynamic shock-wave experiments and static compression in the diamond anvil cell. X-ray diffraction with synchrotron radiation and diamond-anvil cells has extended the range for accurate lattice parameter determinations into the multimegabar region exceeding 300 GPa.[2,3] However, measurements of temperature in shock experiments are extremely difficult for nontransparent materials like iron. The results of different groups on the Hugoniot temperature at a given pressure differ by more than a thousand degrees. Theoretical calculations can help to resolve this issue, but up to now, *ab initio* thermodynamic studies, such as the density-functional theory, the augmented-plane-wave (APW) method,[4] and the quantum-statistical model[5] (QSM) only can give reliable description for cold pressure-volume (P-V) relationship. As for the theoretical calculation of the thermal physical properties, it still remains a great challenge to us.[6,7]

The study of the temperature dependence of the properties of materials requires a proper account of nuclear motions and thermal excitation of electrons. For the contribution of electrons, it can be well considered by using the Fermi gas theory with the electronic density of states calculated from *ab initio* methods.[8] And for simplicity, in this paper, we focus on the contributions of ions to thermodynamic properties. The basic difficulty in the systematic theoretical calculation of the thermodynamic properties of a substance by means of statistical physics is how to correctly incorporate the structurally complicated interatom interaction of the many-body problems.[7] Although some theoretical methods have been developed, substantial uncertainties or difficulties exist. For the most commonly used Debye-Grüneisen (DG) model,[9] which separates the thermal contributions from the zero-temperature equation of state (EOS), explicit anharmonic contributions have been worked out, but the anharmonic contributions have been shown being very important at high temperature.

The cell model is a mean-field approximation to the thermal contribution of atoms to the Helmholtz free energy of crystalline phases.[1,10–13] The model assumes that each atom is confined to the Weigner-Seitz (WS) cell formed by its nearest neighbors. Although interatomic correlations are neglected, the cell model includes anharmonic terms which are important for high temperatures, but which are ignored in the DG model and quasiharmonic lattice dynamics. Many authors have demonstrated that the cell model matches successfully the thermodynamic properties of the fcc Lennard-Jones crystal[11,12] and sodium chloride[13] calculated from Monte Carlo simulations. Wasserman and Stixrude further applied the cell model to a metallic solid iron.[1] The calculated properties are in good agreement with available static and shock-wave experimental measurements.

In terms of the cell model,[1,6,7] the ionic part of Helmholtz free energy of per ion can be written as

$$F(V,T) = E_c(R) - kT[(3/2)\ln(2\pi\mu kT/h^2) + \ln v_f], \quad (1)$$

$$v_f = 4\pi \int_0^{r_m} \exp[-g(r,V)/kT] r^2 dr, \quad (2)$$

where $E_c(R) \equiv E_c(V)$ is the 0-K total energy of per ion. It should be a function of volume V, but also can be seen as a function of the nearest distance R. V is the specific volume of per ion, r_m is the WS radius, $V = R^3/\gamma_0 = 4\pi r_m^3/3$, γ_0 is the structure constant as shown in Eqs. (20) and (22), μ is the weight of the lattice ion, $g(r,V)$ is the mean-field potential[6,7] (MFP), and r corresponds the distance of a single atom displaced from its equilibrium position, while all the other atoms remain in equilibrium. The central issue of the mean-field theory is how to calculate the MFP $g(r,V)$. In this regard, the free-volume theory[11,12] (FVT) was chosen to calculate the MFP by the average of the empirically derived pairwise potentials, and this point substantially limited its application to metallic materials while the tight-binding total-energy (TBTE) classical cell model was chosen to calculate the MFP by the tight-binding total-energy method for which the parameters were determined by the first-principles linearized APW calculation.[1] Because the MFP calculation in the TBTE model also is very time consuming and inconvenient, in a series of recent papers, Wang *et al.* proposed a classical analytic MFP (WAMFP).[6,7,14–19] They think that for a crystal with the inversion symmetry, one can imagine that the vibration of the lattice ion is symmetrical with respect to its equilibrium position; i.e., the MFP seen by the lattice ion should be invariant under the inversion operation. Based on the physical consideration, they constructed the following analytic WAMFP:

$$g(r,V) = \frac{1}{2}[E_c(R+r) + E_c(R-r) - 2E_c(R)] + \frac{\lambda r}{2R}[E_c(R+r) - E_c(R-r)]. \quad (3)$$

Wang *et al.* further demonstrated the reasonability of Eq. (3) by the fact that the three commonly used expressions for the Grüneisen parameter γ_G—i.e., that due to Slater ($\lambda=-1$), that due to Dugdale and MacDonald ($\lambda=0$), and that for the FVT ($\lambda=1$)—can all be explicitly deduced if one takes the second-order approximation to Eq. (3). In this work, we will consider two cases corresponding to $\lambda=0$ and 1. The WAMFP model had been applied to 14 typical metals (Al, Cu, Ta, Mo, W, Ce, Fe, MgO, Be, Pt, Au, W, Th, and U),[6,7,14–19] indicating that both the calculated Hugoniot states and 293-K isotherms fell well in the experimental uncertainties.

In terms of Wang's works and the statement cited above, we postulate that Wang *et al.* believe that their WAMFP is a new physical model being different with and independent to the FVT and TBTE models. However, in this paper, we developed a generalized AMFP (GAMFP) in terms of the nearest-neighbor FVT. And we show that in physical essence, the WAMFP is equivalent to the GAMFP, and in a mathematic aspect, it only is an approximate edition of the GAMFP based on the trapezoid integration formula. Although the approximation is roughest, the numerical results for the nearest-neighbor Lennard-Jones (NN-LJ) model solid show that the agreement of the WAMFP with the integrated GAMFP is fairly good. It has been shown by many authors that the Vinet EOS has fairly good precision for many practical solids than many other EOS with more complicated form.[20–23] In many of the works of Wang *et al.*, they also have fitted their *ab initio* cold energy data $E_c(R)$ by using the Morse potential[6] or analytic expression from modified Vinet EOS (Ref. 19) and further applied the fitted expressions to evaluate thermal contribution. Thus we apply the GAMFP and WAMFP to Vinet EOS to check the applicability of the AMFP to practical solids.

In many works on practical EOS, only the classical cases have been considered for the complication of disposing quantum effects or used the Einstein or Debye models with constant characteristic temperature (Θ_E or Θ_D) and Grüneisen parameter (γ_G) to approximately consider the quantum modification.[20,24,25] However, such a disposition is a rough approximation; it only is applicable to low-compression range or low-pressure conditions. In order to extend the applicable range of Einstein and Debye models, various semiempirical expressions have been developed for Θ_E, Θ_D, and γ_G (Refs. 26–28). In 1942, Pitzer and Gwinn (PG) proposed a semiempirical method to consider the quantum modification of a classical system.[29] And in recent years, the PG method has been applied to many molecular systems with anharmonic interaction.[30,31] Several years ago, Hardy, Lacks, and Shukla (HLS) firstly applied modified PG (mPG) method to consider the quantum modification for Monte Carlo (MC) simulation of a classical solid system without mentioning Pitzer and Gwinn's work.[32] However, after the work of Hardy *et al.*, works using the mPG method to solids are scarce. The reason may be is that the mPG method is firstly proposed for a classical molecular dynamic simulation, yet it is difficult to obtain the quantum modifications in the MD simulation. But an analytic EOS with some approximation is favorable in practice, such as the DG-type EOS, and people have not noticed the strength of mPG method for improving these analytic EOS.

In one of our recent works,[33,34] we reformulated the PG method with explicit physical meanings. It is shown that the quantum effect is important at low temperature, and it can be disposed under the harmonic framework. The anharmonic effect is important at high temperature and tends to zero at low temperature, and it can be disposed by using a classical approximation. The alternative formulation is easier for various applications and has been applied to a Debye-Grüneisen solid with the generalized LJ intermolecular interaction. The expressions for the Debye temperature and Grüneisen parameter as a function of volume are analytically derived. The analytic equation of state is applied to predict the thermodynamic properties of solid xenon at normal pressure with the nearest-neighbor Lennard-Jones interaction and is further applied to predict the properties of solid xenon and krypton at high pressure by using an all-neighbor LJ interaction. The theoretical results are in agreement with the experiments. In

this paper, we further apply the mPG method[33,34] combining the GAMFP and WAMFP to Vinet EOS to consider the quantum and anharmonic effects at same time.

The rest of this work is organized as follows. In Sec. II we develop the GAMFP in terms of the nearest-neighbor FVT and verify the equivalence of the WAMFP with the GAMFP. In Sec. III, the GAMFP and WAMFP are applied to NN-LJ model solid. In Sec. IV, the GAMFP and WAMFP are applied to practical solids combining the Vinet EOS and including the quantum effects. In Sec. V, the numerical results are presented and discussed. At last, conclusive remarks are given in Sec. VI.

II. GENERALIZED ANALYTIC MEAN-FIELD POTENTIAL

Suppose the pairwise potential function is $\varepsilon(r)$. In terms of the free-volume theory and only considering the contribution of nearest neighbors,[8–13,34] the MFP can be expressed as

$$g(r,V) = \delta[\overline{\varepsilon(R,r)} - \overline{\varepsilon(R,0)}], \tag{4}$$

where δ is the number of nearest neighbors and $\overline{\varepsilon(R,r)}$ is the average potential over the solid angle:

$$\overline{\varepsilon(R,r)} = \frac{1}{4\pi r^2}\int_0^{2\pi}\int_0^{\pi} \varepsilon(|R^2+r^2-2Rr\cos\theta|^{1/2}) r^2 \sin\theta d\theta d\varphi$$
$$= \frac{1}{2}\int_0^{\pi} \varepsilon(|R^2+r^2-2Rr\cos\theta|^{1/2})\sin\theta d\theta. \tag{5}$$

Introducing new variable $t=\cos\theta$, we have[34]

$$\overline{\varepsilon(R,r)} = \frac{1}{2}\int_{-1}^{1} \varepsilon(|R^2+r^2-2Rrt|^{1/2}) dt, \tag{6}$$

and the cold energy of per ion is

$$E_c(R) = \frac{1}{2}\delta\varepsilon(R) = \frac{1}{2}\overline{\delta\varepsilon(R,0)} \tag{7}$$

and

$$E_c(r,t) \equiv E_c(|R^2+r^2-2Rrt|^{1/2}) = \frac{1}{2}\delta\varepsilon(|R^2+r^2-2Rrt|^{1/2}), \tag{8}$$

$$\overline{E_c(R,r)} = \frac{1}{2}\int_{-1}^{1} E_c(|R^2+r^2-2Rrt|^{1/2}) dt \equiv \frac{1}{2}\int_{-1}^{1} E_c(r,t) dt. \tag{9}$$

Substituting Eqs. (7) and (9) into Eq. (4), we obtain the following GAMFP:

$$g(r,V) = 2[\overline{E_c(R,r)} - E_c(R)] = \int_{-1}^{1} E_c(r,t) dt - 2E_c(R). \tag{10}$$

We know that Eq. (9) is accurate for the nearest-neighbor model solids; however, its application to practical solids is approximate. The range of interatom interaction of a solid is shorter; the applicability of the approximation is better. And for the solids containing long-range interatom interactions, such as alkali halides, the applicability maybe worsens.

Considering that the integral contained in Eq. (9) is inconvenient for practical applications, we may develop analytic approximate expressions for MFP. And it is to be shown that the WAMFP only is the roughest approximation of Eq. (9). For simplicity, we introduce following shortened notations:

$$E_c(r,1) = E_c(R-r), \quad E_c(r,-1) = E_c(R+r),$$
$$E_c(r,t_0) = E_c(R), \quad t_0 = r/2R. \tag{11}$$

If we approximate the function $E_c(r,t)$ in Eq. (9) by the piecewise linear function

$$E_c(r,t) = \begin{cases} \dfrac{1}{2(1+t_0)}\{[E_c(r,t_0)+t_0E_c(r,-1)]+[E_c(r,t_0)-E_c(r,-1)]t\} & (-1\leqslant t\leqslant t_0), \\ \dfrac{1}{2(1-t_0)}\{[E_c(r,t_0)-t_0E_c(r,1)]-[E_c(r,t_0)-E_c(r,1)]t\}, & (t_0\leqslant t\leqslant 1), \end{cases} \tag{12}$$

we obtain an AMFP under the simplest trapezoid approximation:

$$\overline{E_c(R,r)} \approx \frac{1}{4}[(1+t_0)E_c(r,-1)+(1-t_0)E_c(r,1)] + \frac{1}{2}E_c(R), \tag{13}$$

$$g(r,V) \approx \frac{1}{2}\left[\left(1+\frac{r}{2R}\right)E_c(R+r)+\left(1-\frac{r}{2R}\right)E_c(R-r)\right] - E_c(R). \tag{14}$$

By comparing Eq. (14) with Eq. (3), it is obvious that Eq. (14) just is the WAMFP with $\lambda=1/2$. In Wang's works and

our following practical calculations, it is shown that the difference of numerical results for thermodynamic quantities from the WAMFP with $\lambda=0$, $1/2$, 1, respectively, is very little and the WAMFP can be seen as equivalent to the GAMFP. We would develop another AMFP in terms of the parabola approximation. Replacing the function $E_c(r,t)$ in Eq. (10) by the quadratic function

$$E_c(r,t) \approx a_0 + a_1 t + a_2 t^2, \tag{15}$$

we obtain

$$g(r,V) \approx \frac{1}{3}\left[\left(1+\frac{r}{R}\right)E_c(R+r) + \left(1-\frac{r}{R}\right)E_c(R-r) - 2E_c(R)\right]. \tag{16}$$

The concrete derivation of Eq. (16) is given in Appendix A. By comparing Eq. (16) with Eqs. (3) and (14), it is obvious that the form of Eq. (16) just is similar to the WAMFP with $\lambda=1$, except the prefactor $1/3$ in Eq. (16) is different from $1/2$ in Eqs. (3) and (14).

From the above derivations, we can see that one can develop many AMFP's with different extents of the approximation. For clarity, we do not give more. And in following sections, we will distinguish the integrated GAMFP (exact), WAMFP with $\lambda=0$ and 1 (trapezoid approximation of the GAMFP), and parabola approximation of the GAMFP, Eq. (16), by using the subscripts $i=1,2,3$, respectively. The harmonic approximation for the three AMFP can be derived as follows:

$$g_i(x,V) \approx \begin{cases} (1/3)c(V)R^{-2}r^2, & \text{for } i=1,3, \\ (1/2)c(V)R^{-2}r^2, & \text{for } i=2, \end{cases}$$

$$= \frac{1}{12}\left[5+(-)^i\right]c(V)R^{-2}r^2$$

$$\equiv \frac{1}{2}\mu\omega_i^2 r^2, \quad i=1,2,3, \tag{17}$$

where μ is atomic weight, ω_i is the harmonic frequency of atom, and

$$c(V) = \left[E_c''(R) + \frac{2\lambda}{R}E_c'(R)\right]R^2, \tag{18a}$$

$$\lambda = 1, \text{ for } i=1,3, \quad \lambda = 0,1, \text{ for } i=2. \tag{18b}$$

Equations (17) and (18) show that the WAMFP gives out an incorrect strength coefficient and thus different values of vibrating characteristic temperature as compared with the GAMFP, but all three expressions can give the same Grüneisen coefficient.

III. APPLICATION TO A NEAREST-NEIGHBOR LENNARD-JONES MODEL SOLID

In order to check the equivalence of the WAMFP with the GAMFP, we would apply the above formalism to the NN-LJ model solid, for the solid the GAMFP given in Eq. (10) is accurate. The LJ potential is as follows:

$$\varepsilon(r) = \varepsilon_0\left[\left(\frac{r_e}{r}\right)^{12} - 2\left(\frac{r_e}{r}\right)^6\right]. \tag{19}$$

Introducing the reduced variables and notations

$$V = R^3/\gamma_0, \quad V^* = r_e^3/\gamma_0, \quad \Lambda^* = \delta\varepsilon_0, \tag{20}$$

$$x = r/R, \quad x_m = [3/(4\pi\gamma_0)]^{1/3}, \tag{21}$$

where δ and γ_0 are structural constants,[33,34]

$$\delta = 12 \text{ (fcc)}, \ 8 \text{ (bcc)},$$
$$\gamma_0 = \sqrt{2} \text{ (fcc)}, \ 3\sqrt{3}/4 \text{ (bcc)}, \tag{22}$$

we have

$$E_c(R) = \frac{1}{2}\delta\varepsilon_0\left[\left(\frac{r_e}{R}\right)^{12} - 2\left(\frac{r_e}{R}\right)^6\right] = \frac{1}{2}\Lambda^*\left[\left(\frac{V^*}{V}\right)^4 - 2\left(\frac{V^*}{V}\right)^2\right], \tag{23}$$

and in terms of Eqs. (8), (10), (3), and (16), we obtain

$$g(r,V) \equiv g_i(x,V) = \Lambda^*\left[L_i(x)\left(\frac{V^*}{V}\right)^4 - 2M_i(x)\left(\frac{V^*}{V}\right)^2\right], \tag{24}$$

where the nondimensional auxiliary functions $L_i(x)$ and $M_i(x)$ for three cases with subscripts $i=1,2,3$ are given in Appendix A. Defining the nondimensional free volume $\bar{v}_f$ and comparing with Eq. (2), we obtain

$$v_f \equiv 4\pi r_m^3 \bar{v}_f = 3V\bar{v}_f, \tag{25}$$

$$\bar{v}_f = \int_0^{x_m} \exp[-g_i(x,V)/kT]x^2 dx = \int_0^{x_m} \exp\left\{-\left(\frac{\Lambda^*}{kT}\right)\left[L_i(x)\left(\frac{V^*}{V}\right)^4 - 2M_i(x)\left(\frac{V^*}{V}\right)^2\right]\right\}x^2 dx. \tag{26}$$

In terms of thermodynamic relationships, we can easily derive the analytic EOS and the expressions for other thermodynamic properties. The EOS is as follows:

$$P = -\left(\frac{\partial F}{\partial V}\right)_T = P_c(V) + P^*(T,V), \tag{27}$$

where $P_c(V)$ is the cold pressure, $P^*(T,V)$ is the thermal pressure,

$$P_c \equiv P_c(V) = -\left(\frac{\partial E_c}{\partial V}\right)_T = \frac{\Lambda^*}{V^*}\left[2\left(\frac{V^*}{V}\right)^5 - \left(\frac{V^*}{V}\right)^3\right], \tag{28}$$

$$P^* \equiv P^*(T,V) = \frac{kT}{V}\left[1 + \frac{1}{\bar{v}_f}V\frac{\partial \bar{v}_f}{\partial V}\right], \tag{29}$$

$$V\frac{\partial \bar{v}_f}{\partial V} = -\frac{1}{kT}\int_0^{x_m} V\frac{\partial g_i(x,V)}{\partial V}\exp[-g_i(x,V)/kT]x^2dx, \tag{30}$$

$$V\frac{\partial g_i(x,V)}{\partial V} = 4\Lambda^*\left[L_i(x)\left(\frac{V^*}{V}\right)^4 - M_i(x)\left(\frac{V^*}{V}\right)^2\right]. \tag{31}$$

The expressions for internal energy U and excess internal energy U_E are as follows:

$$U = F - T\left(\frac{\partial F}{\partial T}\right)_V = \frac{3}{2}kT + \frac{kT}{\bar{v}_f}\cdot T\frac{\partial \bar{v}_f}{\partial T} \equiv \frac{3}{2}kT + U_E, \tag{32}$$

$$U_E = \frac{\Lambda^*}{\bar{v}_f}\int_0^{x_m} g_i(x,V)\exp[-g_i(x,V)/kT]x^2dx. \tag{33}$$

The thermal capacity with constant volume is as follows:

$$C_V = \left(\frac{\partial U}{\partial T}\right)_V = \frac{3}{2}k + k\left(\frac{\Lambda^*}{kT}\right)^2\left[-\left(\frac{U_E}{\Lambda^*}\right)^2 + \frac{1}{\bar{v}_f}Q(T,V)\right], \tag{34}$$

$$Q(T,V) = \int_0^{x_m} g_i^2(x,V)\exp[-g_i(x,V)/kT]x^2dx. \tag{35}$$

For simplicity, we further introduce the reduced variables

$$T_r = \frac{kT}{\Lambda^*}, \quad V_r = \frac{V}{V^*}, \quad P_r = \frac{P^*V^*}{\Lambda^*}, \tag{36}$$

$$F_r = \frac{F_E}{\Lambda^*} = -\frac{kT}{\Lambda^*}\ln\bar{v}_f, \quad U_r = \frac{U_E}{\Lambda^*}, \quad C_{Vr} = \frac{C_V}{k}, \tag{37}$$

where F_E the is excess Helmholtz free energy.

IV. APPLICATION TO THE VINET EQUATION OF STATE INCLUDING QUANTUM MODIFICATION

In this section, we will apply the AMFP method to the Vinet EOS (Refs. 20–23) including quantum modification.[33,34] In many of Wang's and other relevant works, only the classical case was considered. In order to obtain thermodynamic properties in whole temperature ranges, one must consider the quantum modifications at low temperature condition. The EOS should be formulated as

$$P = P_c(V) + P^*(T,V) + P_q(T,V), \tag{38}$$

where the equations for $P^*(T,V)$ are the same as Eqs. (38) and (39). $P_q(T,V)$ is the quantum modification; it can be evaluated by using the mPG method[33,34] and Debye-Grüneisen approximation, and its expression will be given in the following. As for the cold pressure, the Vinet EOS gives[20–23]

$$P_c(V) \equiv P_c(R) = 3B_0\frac{(1-y)}{y^2}\exp[\eta(1-y)], \tag{39}$$

$$y = (R/R_0) = (V/V_0)^{1/3}, \quad \eta = \frac{3}{2}(B_0' - 1), \tag{40}$$

where the subscript "0" represents zero temperature and zero pressure. V is the volume, B is the bulk modulus, and B' is the derivative of B with respect to pressure. In order to derive the analytic expression of MFP, we should derive cold energy for Vinet EOS

$$E_c(R) = \frac{3B_0V_0}{\eta^2}(\eta - 1 - \eta y)\exp[\eta(1-y)]. \tag{41}$$

Introducing the new variable

$$s = R_0^{-1}|R^2 + r^2 - 2Rrt|^{1/2} = y|1 + x^2 - 2xt|^{1/2}, \tag{42}$$

the average cold energy can be evaluated as follows:

$$\overline{E_c(R,r)} = \frac{1}{2y^2x}\int_{y(1-x)}^{y(1+x)} E_c(R_0s)sds = \frac{3B_0V_0}{2\eta^4y^2x}[f(s_+) - f(s_-)], \tag{43}$$

where

$$f(s) = [\eta^2s^2 + (3-\eta)(\eta s + 1)]\exp[\eta(1-s)], \tag{44}$$

$$s_+ = y(1+x), \quad s_- = y(1-x). \tag{45}$$

Thus the GAMFP for a Vinet solid can be evaluated:

$$g_1(x,V) = 2[\overline{E_c(R,r)} - E_c(R)]. \tag{46}$$

Correspondingly, the WAMFP can be expressed as

$$g_2(x,V) = \frac{1}{2}[(1+x)E_c(R_0s_+) + (1-x)E_c(R_0s_-) - 2E_c(R)]. \tag{47}$$

The derivatives of the AMFP with respect to the volume needed for Eqs. (38) and (39) can be derived as

$$V\frac{\partial g_i(x,V)}{\partial V} = \frac{y}{3}\frac{\partial g_i(x,V)}{\partial y}, \tag{48}$$

$$y\frac{\partial g_1(x,V)}{\partial y} = -4\overline{E_c(R,r)} + \frac{1}{y^2x}[s_+^2E_c(R_0s_+) - s_-^2E_c(R_0s_-)] + 6P_c(R)V_0y^3, \tag{49}$$

$$y\frac{\partial g_2(x,V)}{\partial y} = -\frac{3}{2y}[s_+^4P_c(R_0s_+)V_0 + s_-^4P_c(R_0s_-)V_0] + 3P_c(R)V_0y^3. \tag{50}$$

In terms of the DG approximation, the quantum modification $P_q(T,V)$ can be expressed as

$$P_q(T,V) = \frac{\gamma_G}{V}(E_D^* - E_{Dcl}^*), \tag{51}$$

$$E_{Dcl}^* = 3kT, \tag{52}$$

where E_D^* is the thermal energy under the quantum harmonic approximation and E_{Dcl}^* is its classical limitation. In the

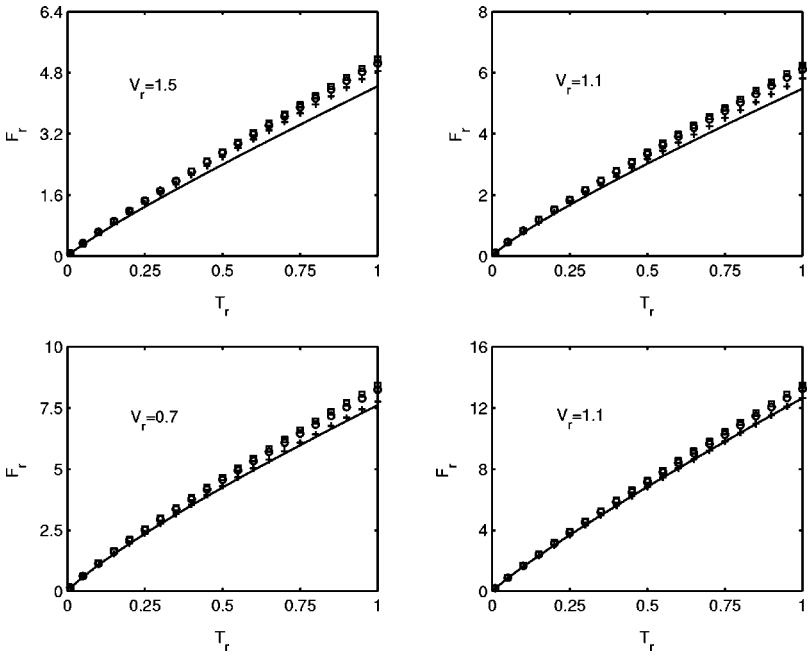

FIG. 1. Variation of reduced excess free energy F_r versus reduced temperature T_r for a classical nearest-neighbor Lennard-Jones model solid at four reduced volumes $V_r=1.5$, 1.1, 0.7, 0.3. Lines: exact expression Eq. (10). Circles: WAMFP with $\lambda=1$. Squares: WAMFP with $\lambda=0$. Crisscrosses: approximate expression, Eq. (16).

original DG approximation, the calculation of E_D^* involves integration. In Appendix B, we develop an analytic expression and E_D^* can be analytically evaluated by using Eq. (B8). As for the Debye characteristic temperature, it can be determined by Eq. (17),

$$\Theta_{Di}=\frac{4}{3}\Theta_{Ei}=\frac{4\hbar\omega_i}{3k}=\frac{2\hbar}{9kR}\sqrt{6[5+(-)^i]c(V)/\mu}, \quad (53)$$

where, for simplicity, we only consider the case with $\lambda=1$ for the WAMFP (as $i=2$), and

$$c(V)=-3\frac{\partial}{\partial y}(y^4P_cV_0)=9B_0V_0y[(\eta+3)y-\eta y^2-2]\times\exp[\eta(1-y)], \quad (54)$$

$$y\frac{\partial}{\partial y}c(V)=-9B_0V_0y[\eta(\eta+6)y^2-\eta^2y^3-(4\eta+6)y+2]\times\exp[\eta(1-y)], \quad (55)$$

and the expressions of Grüneisen coefficient for three cases are the same and can be derived as

$$\gamma_G=-\frac{V}{\Theta_D}\frac{\partial\Theta_D}{\partial V}=\frac{1}{3}-\frac{1}{6}\frac{y}{c(V)}\frac{\partial c(V)}{\partial y}=\frac{[\eta(\eta+4)y^2-\eta^2y^3-2\eta y-2]}{6[(\eta+3)y-\eta y^2-2]}. \quad (56)$$

Supposing $y=1$, we obtain expressions for Θ_D and γ_G at zero pressure:

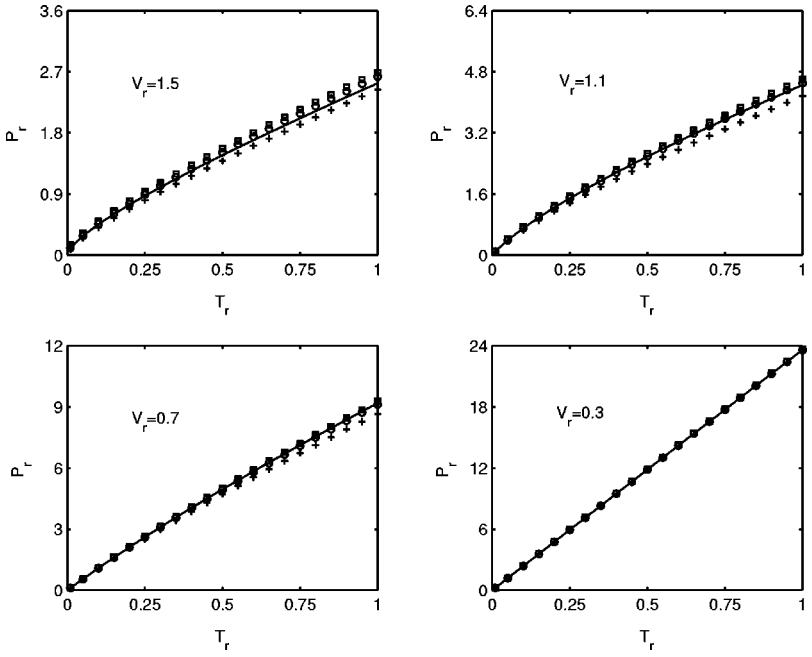

FIG. 2. As for Fig. 1, but for reduced pressure P_r.

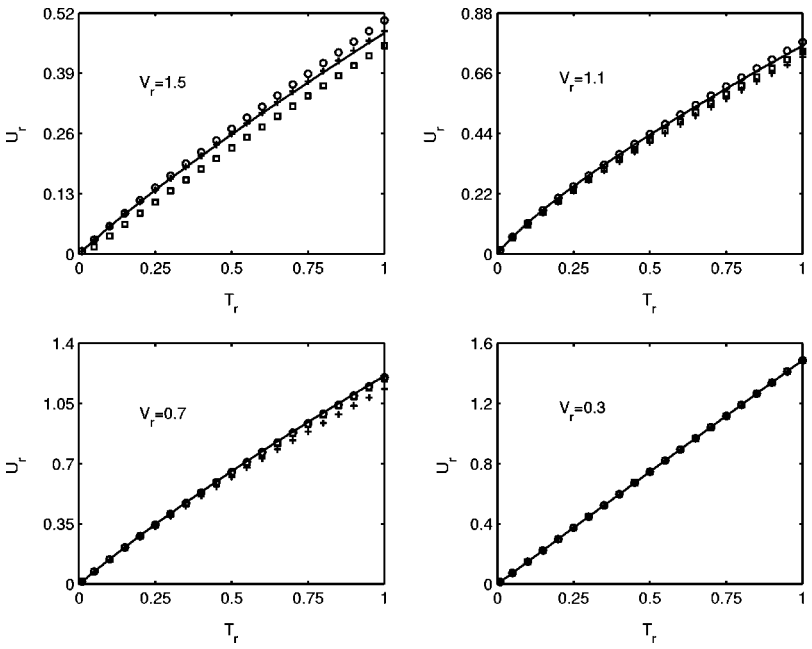

FIG. 3. As for Fig. 1, but for reduced excess internal energy U_r.

$$\Theta_{D0i} = \frac{2\hbar}{3kR_0}\sqrt{6[5+(-)^i]B_0V_0/\mu} \quad (y=1), \tag{57a}$$

$$\Theta_{D0i} = 182.67 \times \{[5+(-)^i]B_0V_{0m}/\mu_m\}^{1/2}(\gamma_0 V_{0m})^{-1/3}\ (\mathrm{K}), \tag{57b}$$

$$B_0 \cdots \mathrm{GPa}, \quad V_{0m} \cdots \mathrm{cm^3\ mol^{-1}}, \quad \mu_m \cdots \mathrm{g\ mol^{-1}}, \tag{57c}$$

$$\gamma_{G0} = (3B_0' - 5)/6 \quad (y=1). \tag{58}$$

V. NUMERICAL RESULTS AND DISCUSSION

In order to check the accuracy of three approximate expressions of the AMFP, we have made comparative calculations for the variation of F_r, P_r, U_r, and C_{Vr} of the NN-LJ model solid versus T_r by using the equations derived previously. The results are depicted in Figs. 1–4. For all calculations, we have considered four cases with reduced volumes V_r=1.5, 1.1, 0.7, and 0.3, respectively. In terms of the EAM results, the potential depth (ε_0/k) of pairwise potential for most metals about ranges from 1000 to 2000 K, and the 10 000 K approximately corresponds to the range of T_r as (0.5–1). So our calculations have been made for the range of T_r within (0–1).

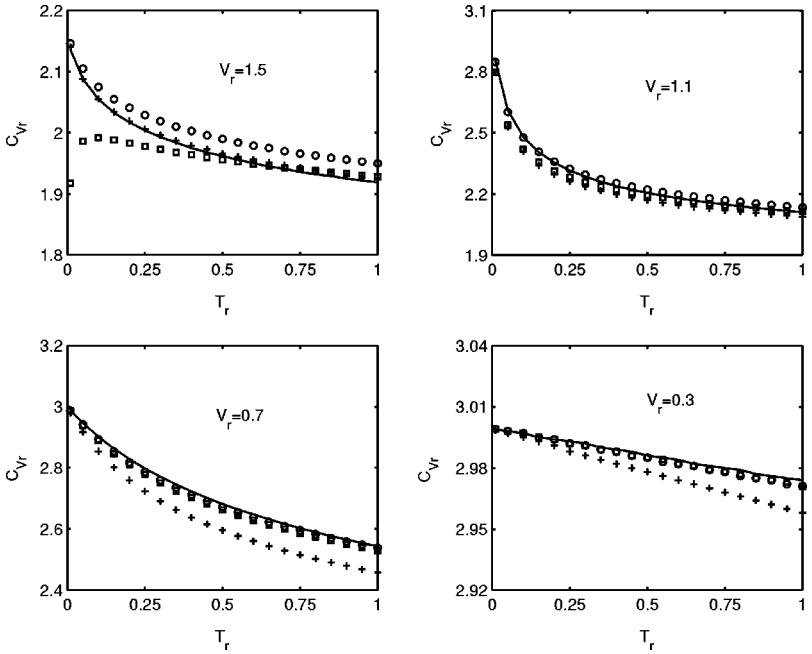

FIG. 4. As for Fig. 1, but for reduced capacity at constant volume C_{Vr}.

TABLE I. Comparison of experimental data with calculated results for the Grüneisen parameters (γ_G), Debye characteristic temperature (Θ_D), and bulk thermal expansivity (α_T) at a reference temperature (T_{ref}) and zero pressure. Cal. 1: exact AMFP with quantum modification. Cal. 2: WAMFP with $\lambda=1$ and quantum modification. Cal. 3: quantum harmonic DG approximation. Cal. 4: classical WAMFP with $\lambda=1$. The experimental data used in the table are taken from Ref. 25.

	γ_G		Θ_D (K)				$\alpha_T(T_{ref})$ (10^{-6} K^{-1})				
Solid	Exp.	Cal.	Exp.	Cal. 1	Cal. 2	T_{ref}	Exp.	Cal. 1	Cal. 2	Cal. 3	Cal. 4
Ar	2.7	2.92	92	76.9	94.2	40	1068	1649	1622	1482	1832
Kr	2.8	2.82	71.9	56.5	69.1	60	904	1224	1206	1266	1276
Xe	2.8	3.07	64	51.7	63.3	60	600	835	826	869	868
NaCl	1.59	1.84	321	212	260	298	120	72.79	72.63	73.74	75.22
LiF	1.63	1.78	735	453	554	300	99.6	57.22	57.27	55.58	71.90
NaF	1.52	1.81	489	318	390	300	98.1	63.23	63.15	63.29	68.01
KCl	1.41	1.89	235	171	209	300	110.8	73.78	73.59	75.19	75.31
CsCl	2.03	2.09	151	114	140	300	141	74.96	74.72	77.18	75.60
Li	0.878	0.922	344	383	469	294	139.8	137.8	137.7	134.9	154.0
Na	1.24	1.23	159	168	206	294	213	203.7	202.8	208.2	208.1
K	1.24	1.27	90.7	100	123	297	236	224.3	223.2	234.7	225.9
Rb	1.26	1.24	56	62	75.9	295	270	226.0	224.9	238.5	226.4
Cs	1.14	1.10	38.7	44.7	54.7	270	290	211.8	211.1	220.9	212.1
Al	2.16	1.74	431	453	555	300	69.7	51.91	51.93	51.27	60.79
Fe	1.66	2.16	472	458	561	300	35.1	41.93	41.94	41.54	48.68
Cu	2.00	1.99	344	377	462	300	50.4	48.36	48.34	48.15	53.98
Zn	1.90	1.62	327	278	341	300	89.1	64.81	64.73	65.03	68.66
Ag	2.35	2.27	227	226	326	300	57.6	53.85	53.75	54.23	56.90
Cd	2.20	2.55	209	197	242	300	94.5	104.3	103.8	108.0	107.0
Pt	2.63	1.97	238	323	396	300	26.8	17.90	17.91	17.94	19.48
Au	2.99	2.42	162	255	312	300	42.5	34.06	34.02	34.28	35.87
Pb	2.60	2.02	105	137	168	300	86.7	64.76	64.60	66.10	65.70

Figure 1 shows that the agreement of the reduced free energy calculated from three approximate expressions is in good agreement with the exact one, but the approximate expression, Eq. (16), is slightly better than the WAMFP. Figures 2–4 show that the cases for reduced pressure, excess internal energy, and thermal capacity, the WAMFP with $\lambda=1$ gives the best agreement with the exact one. But one exception occurred for the WAMFP with $\lambda=0$, which is for the thermal capacity with low density $V_r=1.5$, the tendency as temperature tends to zero is incorrect. In other conditions, the WAMFP with $\lambda=0$ and 1 gives equivalently good results for all four physical quantities. And we can postulate that approximate expression, Eq. (14), corresponding to the WAMFP with $\lambda=1/2$ must give equivalently good results. Thus one can conclude that the WAMFP indeed is equivalent to the GAMFP, Eq. (10), and also is equivalent to free-volume theory with nearest-neighbor interactions.

In order to check the applicability of several AMFP expressions, we apply the formalism developed in Sec. IV to three types of solids, including rare-gas, alkali-halide, and metallic solids. In Table I, the calculated results for the Grüneisen parameters (γ_G), Debye characteristic temperature (Θ_D), and volume thermal expansivity (α_T) at the reference temperature (T_{ref}) and zero pressure are compared with experimental data. The experimental data listed in the table are taken from Ref. 25. For α_T, we considered four cases. The first case is the exact AMFP, Eq. (10), with quantum modification; the second case is the WAMFP with $\lambda=1$ and with quantum modification; the third case is the quantum harmonic DG approximation; and the fourth case is the classical WAMFP with $\lambda=1$. For Θ_D, we only considered first and second cases. The table shows that for 22 typical materials, the calculated γ_G only is qualitatively in agreement with the experimental data. For rare-gas and alkali-halide solids, the agreement of calculated values of Θ_D with experimental data for case 2 is better than case 1. But for metallic solids, case 1 is better than case 2. Because case 1 belongs to a strict nearest-neighbor GAMFP, case 2 is the WAMFP in Eq. (3), for which the prefactor $1/2$ in Eq. (3) is different from $1/3$ in Eq. (16), because the value $1/3$ just corresponds to the harmonic approximation of GAMFP and $1/2$ can be seen as a compensate corresponding to non-nearest neighbors for the WAMFP. We can postulate from the results of Θ_D that the non-nearest interaction is more important for rare-gas and alkali-halide solids than metallic solids. Such a situation shows that the pairwise interaction between metallic atoms must be short range and this is in agreement with the NN-EAM potential for metallic solids developed by Baskes.[35,36] Although the NN-EAM potential is fairly simple, it has been used by many other authors, and it has been shown to explain many properties of metallic solids.[35–39]

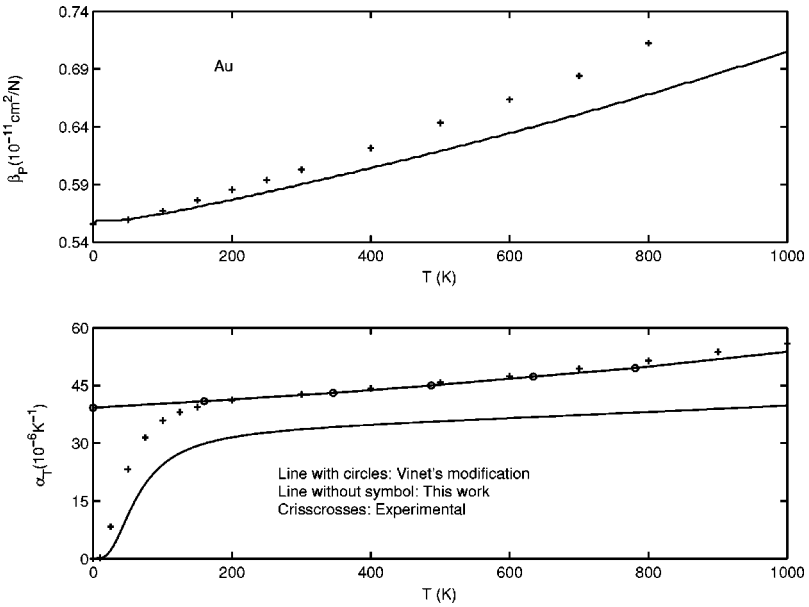

FIG. 5. Variation of compressibility coefficient $\beta_p(10^{-11}\ \mathrm{cm}^2\ \mathrm{N}^{-1})$ and bulk thermal expansivity coefficient $\alpha_T\ (10^{-6}\ \mathrm{K}^{-1})$, at zero pressure versus temperature T for gold. Line with circles: Vinet's modification, line without symbol: this work, crisscrosses: experiment. The experimental data used are taken from Refs. 20, 24–26, and 40. The results of β_p from the Vinet EOS have not been plotted, because Vinet's results almost are completely in agreement with experiment.

Table I also shows that the difference of calculated α_T between four cases is small. The reason maybe is that the reference temperature T_{ref} is high enough to make the classical approximation being applicable, and at these values of T_{ref}, the anharmonic effects are not too obvious. But the agreement of calculated α_T with experimental data is fairly bad for rare-gas and alkali-halide solids. We believe that the reason also is the negligence of non-nearest interactions. Although for metals the agreement is slightly better, only for few metallic solids is the agreement just acceptable. In Figs. 5–8, we plotted the variation of compressibility and thermal expansivity coefficients versus temperature for four typical materials—that is, gold, copper, sodium chloride, and xenon. The experimental data used in these figures are taken from Refs. 20, 24–26, and 40. These figures show that the agreement of the AMFP with experiment is acceptable only for copper, the agreement is overall fairly bad for the other three materials. The situation just is in agreement with Table I. However, the four figures also show that the theoretical results from Vinet's semiempirical modification are in good agreement with the experiment as the temperature being higher than the Θ_D. This is because Vinet's semiempirical modification has used more experiment information, including the experimental data of γ_G, Θ_D, and α_T at some reference temperature.

At last, we point out that the direct application of the AMFP to metallic solids is in contradiction with the EAM.[35–39] In terms of Eqs. (3) and (10) the AMFP uses all cold energy $E_c(R)$ to evaluate $g(r,V)$, and this is equivalent to evaluating thermal part of thermodynamic quantities by using all cold energy. But numerous works[35–39] on the EAM have shown that in order to explain most physical properties of metallic solids, one must divide $E_c(R)$ into two parts. One part is the contribution of free-electron gas; another part is the contribution of pairwise interaction between metallic atoms. This also means that the pairwise interaction between

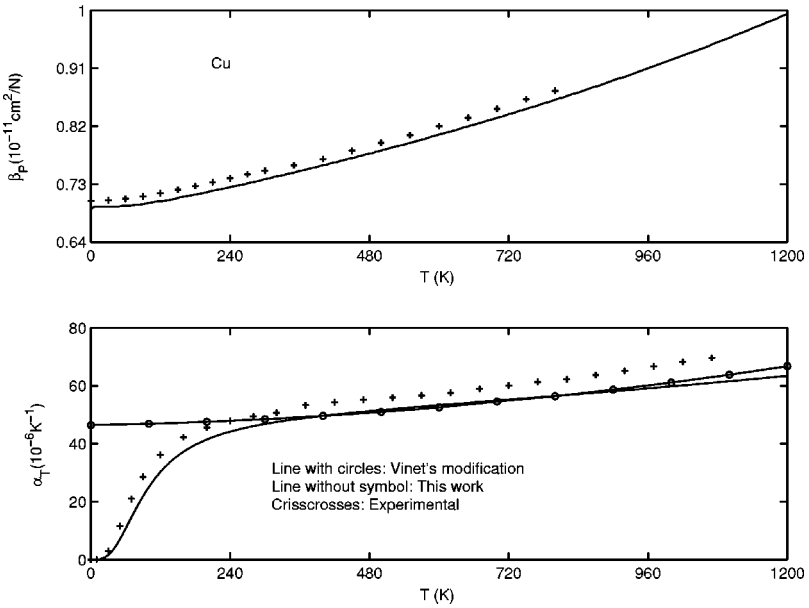

FIG. 6. As for Fig. 5, but for copper.

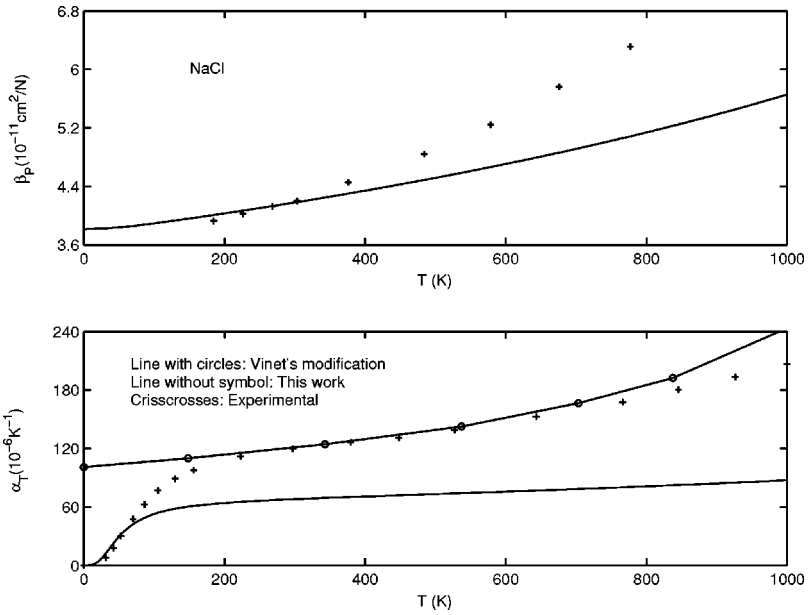

FIG. 7. As for Fig. 5, but for sodium chloride.

metallic atoms must eliminate free-electron gas contribution. For some typical metals, analytic EAM potentials have been established, and very recently, Song and Morris have used these potentials combining the modified Weeks-Chandler-Anderson (mWCA) perturbation theory to research thermodynamic properties of these metals.[39] The good agreement of theoretical results with experimental data shows that the EAM is reasonable. And correspondingly, direct application of the AMFP method to metallic solids is in doubt. Also the good results shown in Wang's works should be carefully appraised. However, it is obvious that the discrepancy between the EAM and AMFP mainly lies in separating the free-electron gas part from the total cold energy. One can easily combine the EAM into the AMFP method and develop an improved model. The unique way needed to do this is to replace the total cold energy $E_c(R)$ in Eqs. (3) and (10) by $E_{c,ion}(R)$, and $E_{c,ion}(R)$ is the contribution of the pairwise interaction between metallic ions to cold energy.

VI. CONCLUSIONS

A GAMFP is established strictly in terms of the free-volume theory and the nearest-neighbor pairwise interaction assumption. By using the numerical integrated formula to evaluate the integral contained in the GAMFP, it is shown that the WAMFP is an approximate analytic version of the GAMFP. The GAMFP is exact for nearest-neighbor model solids. The GAMFP, WAMFP, and other AMFP's with slightly different forms are applied to the classical NN-LJ model solid. The numerical results for four reduced thermodynamic properties—free energy, pressure, excess internal energy, and thermal capacity—show that the numerical results from the WAMFP are almost completely in agreement with the GAMFP and are slightly better than several other approximate AMFP's.

In order to check the applicability of the GAMFP and WAMFP, we applied them to Vinet-type solids for the Vinet

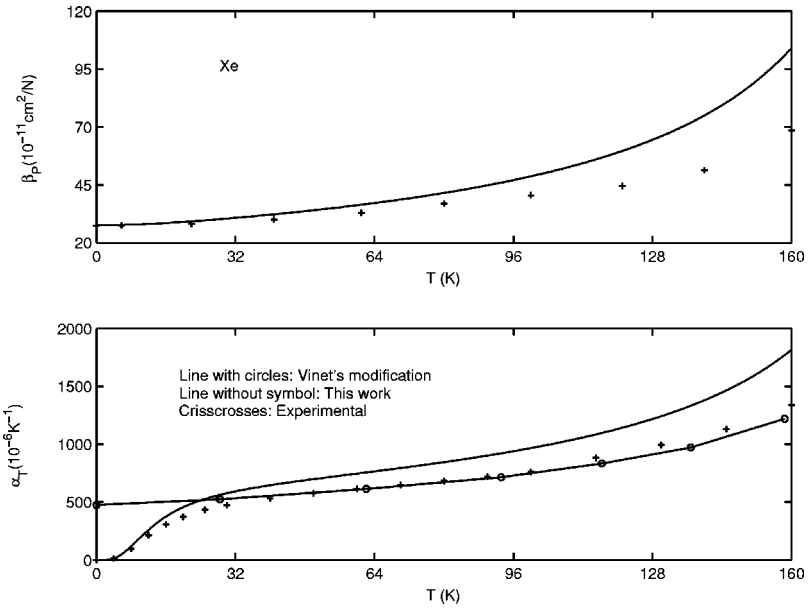

FIG. 8. As for Fig. 5, but for xenon.

equation of state has been shown having a fairly high precision. The quantum modifications have been taken into account by using a modified Pitzer-Gwinn method and DG model. The derivation procedure shows that the WAMFP gives a different expression of the Debye temperature Θ_D but the same expression for the Grüneisen coefficient γ_G as compared with the GAMFP. Thus the WAMFP is equivalent to the GAMFP in the classical case, but not for the quantum case for the difference of Θ_D. However, our numerical calculations show that the difference of thermodynamic quantities from Θ_D is very little.

The numerical results for three types of solids show that the theoretical values of γ_G and Θ_D are qualitatively in agreement with experiments, but the agreement is not satisfactory quantitatively. The predicted values of the bulk thermal expansivity are too large for rare-gas solids, too small for alkali-halide solids, and for metallic solids the agreement is better but also is not satisfactory. Especially the predicted variations of bulk thermal expansivity and compressibility versus temperature are fairly bad; except for copper, the prediction is fortunately acceptable. It is shown that the fundamental spirit of the AMFP to use all cold energy to evaluate thermal properties is in contradiction with the EAM. It is necessary to improve the AMFP in terms of the EAM by the replacement of all cold energy with cold energy from interaction between metallic atoms.

ACKNOWLEDGMENTS

This work was supported by the Joint Fund of NSFC and CAEP under Grant No. 10476007, the Oversea Scholarship Program of UESTC, and the Youth Science and Technology Foundation of UESTC under Grant No. YF020703.

APPENDIX A

In this appendix, we firstly give the derivation of Eq. (16). By substituting Eq. (15) into Eq. (9), we have

$$\overline{E_c(R,r)} \approx a_0 + \frac{1}{3}a_2, \tag{A1}$$

where the coefficients a_0 and a_2 can be solved from the following equations:

$$E_c(r,t_0) = a_0 + a_1 t_0 + a_2 t_0^2,$$

$$E_c(r,1) = a_0 + a_1 + a_2,$$

$$E_c(r,-1) = a_0 - a_1 + a_2, \tag{A2}$$

$$a_0 = \frac{(-t_0)}{2(1-t_0)}E_c(r,1) + \frac{1}{1-t_0^2}E_c(r,t_0) + \frac{t_0}{2(1+t_0)}E_c(r,-1),$$

$$a_2 = \frac{1}{2(1-t_0)}E_c(r,1) - \frac{1}{1-t_0^2}E_c(r,t_0) + \frac{1}{2(1+t_0)}E_c(r,-1). \tag{A3}$$

Substituting Eq. (A3) into Eq. (A1) and combining Eq. (13), one obtains

$$\overline{E_c(R,r)} \approx \frac{1}{6}\left[\frac{(1+3t_0)}{(1+t_0)}E_c(r,-1) + \frac{4}{1-t_0^2}E_c(r,t_0) + \frac{(1-3t_0)}{(1-t_0)}E_c(r,1)\right] \tag{A4}$$

or

$$g(r,V) = \frac{1}{3}\left[\frac{(2R+3r)}{(2R+r)}E_c(R+r) + \frac{(2R-3r)}{(2R-r)}E_c(R-r) - \frac{(8R^2-6r^2)}{(4R^2-r^2)}E_c(R)\right]. \tag{A5}$$

For simplicity, we take the following approximation:

$$\frac{(2R+3r)}{(2R+r)} \approx 1 + \frac{r}{R}, \quad \frac{(2R-3r)}{(2R-r)} \approx 1 - \frac{r}{R}, \quad \frac{(8R^2-6r^2)}{(4R^2-r^2)} \approx 2, \tag{A6}$$

$$g(r,V) \approx \frac{1}{3}\left[\left(1+\frac{r}{R}\right)E_c(R+r) + \left(1-\frac{r}{R}\right)E_c(R-r) - 2E_c(R)\right]. \tag{A7}$$

In our numerical calculations, it is shown that the difference for thermodynamic quantities from the approximation in Eq. (A6) is negligible.

Subsequently, we present the nondimensional auxiliary functions $L_i(x)$ and $M_i(x)$ for three cases with subscripts $i = 1,2,3$:

$$L_1(x) = \frac{1}{20x(1-x)^{10}} - \frac{1}{20x(1+x)^{10}} - 1,$$

$$M_1(x) = \frac{1}{8x(1-x)^4} - \frac{1}{8x(1+x)^4} - 1, \tag{A8}$$

$$L_2(x) = \frac{(1+\lambda x)}{4(1+x)^{12}} + \frac{(1-\lambda x)}{4(1-x)^{12}} - \frac{1}{2},$$

$$M_2(x) = \frac{(1+\lambda x)}{4(1+x)^6} + \frac{(1-\lambda x)}{4(1-x)^6} - \frac{1}{2}, \tag{A9}$$

$$L_3(x) = \frac{1}{6(1+x)^{11}} + \frac{1}{6(1-x)^{11}} - \frac{1}{3},$$

$$M_3(x) = \frac{1}{6(1+x)^{5}} + \frac{1}{6(1-x)^{5}} - \frac{1}{3}. \quad \text{(A10)}$$

APPENDIX B

Now we derive the analytic expression of thermal energy in Eq. (51) under the Debye-Grüneisen approximation. The vibrational Helmholtz free energy under harmonic model is as follows:

$$F_D^* = \frac{1}{2}\int \hbar\omega D(\omega)d\omega + kT\int \ln(1-e^{-\hbar\omega+kT})D(\omega)d\omega, \quad \text{(B1)}$$

where the first term is the zero-point energy and $D(\omega)$ is the state density. Under Debye-Gruüeisen approximation, the state density can be expressed as

$$D(\omega)d\omega = \begin{cases} 9\dfrac{\omega^2}{\omega_D^3}d\omega, & \omega \leqslant \omega_D, \\ 0, & \omega > \omega_D. \end{cases} \quad \text{(B2)}$$

Substituting Eq. (B2) into Eq. (B1) and introducing the notations

$$x = \frac{\hbar\omega}{kT}, \quad \Theta_D = \frac{\hbar\omega_D}{k}, \quad x_D = \frac{\hbar\omega_D}{kT} = \frac{\Theta_D}{T}, \quad \text{(B3)}$$

Eq. (B1) is changed to

$$F_D^* = \frac{9}{8}k\Theta_D + 9kT\left(\frac{T}{\Theta_D}\right)^3\int_0^{x_D}\ln(1-e^{-x})x^2dx. \quad \text{(B4)}$$

The integration contained in Eq. (B4) cannot be evaluated analytically and is inconvenient for practical applications. We would develop an analytic expression in terms of the following expansion:

$$\ln(1-e^{-x}) = \begin{cases} \ln x - \dfrac{1}{2}x + \dfrac{1}{24}x^2 - \dfrac{7}{20160}x^4 & (x \leqslant 1), \\ -\displaystyle\sum_{n=1}^{\infty}\frac{1}{n}e^{-nx} & (x > 1). \end{cases} \quad \text{(B5)}$$

By using Eq. (B5), we can analytically evaluate the integration contained in Eq. (B4):

$$\int_0^{x_D}\ln(1-e^{-x})x^2dx = \frac{1}{3}x_D^3\left(\ln x_D - \frac{1}{3} - \frac{3}{8}x_D + \frac{1}{40}x_D^2 - \frac{1}{6720}x_D^4\right) \quad (x_D \leqslant 1), \quad \text{(B6a)}$$

$$\begin{aligned}\int_0^{x_D}\ln(1-e^{-x})x^2dx &= \int_0^{\infty}\ln(1-e^{-x})x^2dx - \int_{x_D}^{\infty}\ln(1-e^{-x})x^2dx \\ &= -\frac{\pi^4}{45} + \sum_{n=1}^{\infty}\frac{1}{n}\int_{x_D}^{\infty}e^{-nx}x^2dx \\ &\approx -\frac{\pi^4}{45} + \sum_{n=1}^{10}\frac{1}{n^4}[n^2x_D^2 + 2nx_D + 2]e^{-nx_D} \quad (x_D > 1).\end{aligned} \quad \text{(B6b)}$$

Thus Eq. (B4) is changed to the following form:

$$F_D^* = \frac{9}{8}k\Theta_D + 3kT\left[\ln\left(\frac{\Theta_D}{T}\right) - \frac{1}{3} - \frac{3}{8}\left(\frac{\Theta_D}{T}\right) + \frac{1}{40}\left(\frac{\Theta_D}{T}\right)^2 - \frac{1}{6720}\left(\frac{\Theta_D}{T}\right)^4\right] \quad (T \geqslant \Theta_D), \quad \text{(B7a)}$$

$$F_D^* = \frac{9}{8}k\Theta_D - \frac{1}{5}\pi^4kT\left(\frac{T}{\Theta_D}\right)^3 + 9kT\left(\frac{T}{\Theta_D}\right)^3\sum_{n=1}^{10}\frac{1}{n^4}\left[n^2\left(\frac{\Theta_D}{T}\right)^2 + 2n\left(\frac{\Theta_D}{T}\right) + 2\right]\exp\left[-n\left(\frac{\Theta_D}{T}\right)\right] \quad (T < \Theta_D). \quad \text{(B7b)}$$

Correspondingly, the internal energy for an atom is derived as

$$E_D^* = 3kT\left[1 - \frac{3}{8}\left(\frac{\Theta_D}{T}\right) + \frac{1}{20}\left(\frac{\Theta_D}{T}\right)^2 - \frac{1}{1680}\left(\frac{\Theta_D}{T}\right)^4\right] \quad (T \geqslant \Theta_D), \quad \text{(B8a)}$$

$$E_D^* = \frac{9}{8}k\Theta_D + \frac{3}{5}\pi^4kT\left(\frac{T}{\Theta_D}\right)^3 - 9kT\left(\frac{T}{\Theta_D}\right)^3\sum_{n=1}^{10}\frac{1}{n^4}\left[n^3\left(\frac{\Theta_D}{T}\right)^3 + 3n^2\left(\frac{\Theta_D}{T}\right)^2 + 6n\left(\frac{\Theta_D}{T}\right) + 6\right]\exp\left[-n\left(\frac{\Theta_D}{T}\right)\right] \quad (T < \Theta_D). \quad \text{(B8b)}$$

And the heat capacity for an atom is

$$\frac{C_V}{k} = 3\left[1 - \frac{1}{20}\left(\frac{\Theta_D}{T}\right)^2 + \frac{3}{1680}\left(\frac{\Theta_D}{T}\right)^4\right] \quad (T \geqslant \Theta_D), \quad \text{(B9a)}$$

$$\frac{C_V}{k} = \frac{12}{5}\pi^4\left(\frac{T}{\Theta_D}\right)^3 - 9\left(\frac{T}{\Theta_D}\right)^3\sum_{n=1}^{10}\frac{1}{n^4}\left[n^4\left(\frac{\Theta_D}{T}\right)^4 + 4n^3\left(\frac{\Theta_D}{T}\right)^3 + 12n^2\left(\frac{\Theta_D}{T}\right)^2 + 24n\left(\frac{\Theta_D}{T}\right) + 24\right]\exp\left[-n\left(\frac{\Theta_D}{T}\right)\right] \quad (T < \Theta_D). \quad \text{(B9b)}$$

[1] E. Wasserman and L. Stixrude, Phys. Rev. B **53**, 8296 (1996).
[2] Y. K. Vohra and J. Akella, Phys. Rev. Lett. **67**, 3563 (1991).
[3] Y. K. Vohra and W. B. Holzapfel, High Press. Res. **11**, 223 (1993).
[4] J. Hama, K. Suito, and N. Kawakami, Phys. Rev. B **39**, 3351 (1989).
[5] N. N. Kalitkin and L. V. Kuz'mina, Sov. Phys. Solid State **13**, 1938 (1972).
[6] Y. Wang, Phys. Rev. B **62**, 196 (2000).
[7] Y. Wang, D. Chen, and X. Zhang, Phys. Rev. Lett. **84**, 3220 (2000).
[8] C. W. Greeff and M. J. Graf, Phys. Rev. B **69**, 054107 (2004).
[9] V. L. Moruzzi, J. F. Janak, and K. Schwarz, Phys. Rev. B **37**, 790 (1988).
[10] Z. W. Salsburg and W. W. Wood, J. Chem. Phys. **37**, 798 (1962).
[11] F. H. Ree and A. C. Holt, Phys. Rev. B **8**, 826 (1973).
[12] K. Westera and E. R. Cowley, Phys. Rev. B **11**, 4008 (1975).
[13] E. R. Cowley, J. Gross, Zhaoxin Gong, and G. K. Horton, Phys. Rev. B **42**, 3135 (1990).
[14] Y. Wang, Phys. Rev. B **63**, 245108 (2001).
[15] Y. Wang, Phys. Rev. B **61**, R11 863 (2000).
[16] Y. Wang, R. Ahuja, and B. Johansson, Phys. Rev. B **65**, 014104 (2001).
[17] L. Li and Y. Wang, Phys. Rev. B **63**, 245108 (2001).
[18] Y. Wang, R. Ahuja, and B. Johansson, J. Appl. Phys. **92**, 6616 (2002).
[19] Y. Wang, R. Ahuja, and B. Johansson, J. Phys.: Condens. Matter **14**, 7321 (2002).
[20] P. Vinet, J. Ferrante, J. R. Smith, and J. H. Rose, Phys. Rev. B **35**, 1945 (1987).
[21] P. Vinet, J. H. Rose, J. Ferrante, and J. R. Smith, J. Phys.: Condens. Matter **1**, 1941 (1989).
[22] J. Hama and K. Suito, J. Phys.: Condens. Matter **8**, 67 (1996).
[23] E. Brosh, G. Makov, and R. Z. Shneck, J. Phys.: Condens. Matter **15**, 2991 (2003).
[24] M. Taravillo, V. G. Baonza, J. Nunez, and M. Caceres, Phys. Rev. B **54**, 7034 (1996).
[25] M. Taravillo, V. G. Baonza, J. E. F. Rubio, J. Nunez, and M. Caceres, J. Phys. Chem. Solids **63**, 1705 (2002).
[26] G. E. Fernandez, J. Phys. Chem. Solids **59**, 867 (1998).
[27] S. B. Segletes and W. P. Walters, J. Phys. Chem. Solids **59**, 425 (1998).
[28] U. Ponkratz and W. B. Holzapfel, J. Phys.: Condens. Matter **16**, S963 (2004).
[29] K. S. Pitzer and W. D. Gwinn, J. Chem. Phys. **10**, 428 (1942).
[30] Pan Hui-yun, J. Chem. Phys. **87**, 4846 (1987).
[31] G. Taubmann, W. Witschel, and L. Schoendorff, J. Phys. B **32**, 2859 (1999).
[32] R. J. Hardy, D. J. Lacks, and R. C. Shukla, Phys. Rev. B **57**, 833 (1998).
[33] Sun Jiu-Xun, Wu Qiang, Cai Ling-Cang, and Jing Fu-Qian, Chin. Phys. **12**, 632 (2001).
[34] Sun Jiu-Xun, Yang Hong-Chun, Wu Qiang, and Cai Ling-Cang, J. Phys. Chem. Solids **63**, 113 (2002).
[35] M. I. Baskes, Phys. Rev. B **46**, 2727 (1992).
[36] M. I. Baskes, Phys. Rev. B **62**, 15 532 (2000).
[37] J. Cai and Y. Y. Ye, Phys. Rev. B **54**, 8398 (1996).
[38] S. Chantasiriwan and F. Milstein, Phys. Rev. B **58**, 5996 (1998).
[39] X. Y. Song and J. R. Morris, Phys. Rev. B **67**, 092203 (2003).
[40] X. S. Qian, *A Lecture for Physical Mechanics* (in Chinese) (Science Press, Beijing, 1962).